ORIGINAL ARTICLE

Application of Fourier Transform for Analysis of Surface Topographic Properties of Dental Zirconia

Naoyoshi TARUMI[1,2], Tsukasa AKASAKA[1], and Fumio WATARI[1]

.[1]Graduate School of Dental Medicine, Hokkaido University, Sapporo, Japan
[2]Sapporo Dental Laboratory, Sapporo, Japan

Synopsis
The clinical application of dental zirconia has increased. Adhesion on dental zirconia is important in the usage such as the hybrid type abutment to adhesive to titanium cylinder. For the analysis of surface roughness to influence on various material properties, conventionally the value of depth directions such as the Ra has been widely used. However, the periodicity (wavelength) of roughness in the horizontal direction may also influence adhesive property. The Fourier transform that can perform frequency analysis was effective for the examination of a complicated roughness curve, composed of multiple waves. Shear bond strength test was conducted in the specimen with four kinds of surface roughness (control, low, high, low and high frequency element). Shear bond strength became strong (14MPa) in the specimen with a short wavelength (high frequency element), and weak (4~5MPa) for a long wavelength (low frequency element). The surface sensitive properties depend not only on the Ra but also on the wavelength. In this study the Fourier transform was effective for various characteristic examinations of surface properties such as the adhesive property and shear bond strength could be better understood by wavelength dependence.

Key words: *dental zirconia, surface roughness, Fourier transform, shear bond strength, resin cement*

Introduction

Dental zirconia has been used for the application as an internal frame in the beginning [1]. Zirconia begins to be used as dental implant with its good compatibility [2, 3] to both hard tissue [4] and soft tissue [5].

Recently, applied cases have been enlarged, such as the hybrid type abutment to adhesive titanium cylinder, and the titanium base screw retained zirconia crown. In those cases the fewer adhesion of plaque and higher adhesive strength to resin cement are favored [6, 7]. For the analysis of the influence of surface roughness to influence on various material properties [8], conventionally the value in the depth directions, such as Ra (arithmetic mean roughness) has been used [9]. However, the periodicity (wavelength) of the roughness in the plane direction may have a larger influence, depending on the surface-sensitive properties. In this study, Fourier transform, which enables frequency analysis, was applied for the analysis of the wavelength of the zirconia surface roughness and used for the detection of the roughness level responsible for the resin cement adhesive strength [10,11].

Materials and methods

1. Specimen:

Pairs of small and large plate specimens (12×12×5 mm^3, 18×20×10 mm^3) were made from semi-sintered zirconia (Aadva zirconia disk, GC, Tokyo, Japan) and the surface was smoothed with abrasive paper (#1,500). All zirconia specimens were sintered for 4 hours at 1,500°C and slowly cooled down to 200°C taking for 10 hours. Specimens shrank approximately 20% by sintering (10×10×4mm^3, 14×18×8 mm^3).

2. Surface treatments

Four different types of surface treatment were done for all the specimens. 1) Untreated as control (CTR), 2) 1mm interval groove added by fine diamond bar as low frequency surface roughness (Low), 3)Sandblast treatments (alumina 50 μm, 2 atm) as high frequency surface roughness (High), 4) Sandblast treatments after 1mm interval groove added as low and high frequency (Low+High) (Fig.1).

3. Adhesion

Pairs of plate specimen were bonded after surface roughness and contact angle measurements. Resin cement (BeautiCem SA, Shofu, Kyoto, Japan) was used as adhesive with and without primer treatment (monobond-plus: Ivoclar Vivadent, Principality of Liechtenstein).

4. Analysis

1) Surface roughness: The surface roughness was measured using SURFCOM 1400A (Tokyo Seimitu, Tokyo, Japan) (measurement length: 8500 μm, measurement speed: 60 μm/sec, plotting points: 14168 pts.). For the specimen Low and Low+High, roughness was measured in the vertical direction to the groove.

2) Shear bond strength: Large plate specimens were adjusted to a fixed side, and small plate specimens were used for the test piece as a load side. Compression shear bond strength was measured using a universal testing machine INSTRON model-5584 (Instron, USA) with a load cell of 5kN and a crosshead speed of 1.0 mm/min (Fig.2). After both plates were adhered, the jig was set to press down the side of small plate specimen. For the specimens Low and Low+High, shear test was done in the vertical direction to the groove array (Fig.2b).

3) Wettability: Contact angle was measured using Drop Muster DMs-200 (Kyowa Interface Science, Saitama, Japan) (n=10) (Fig.3). For

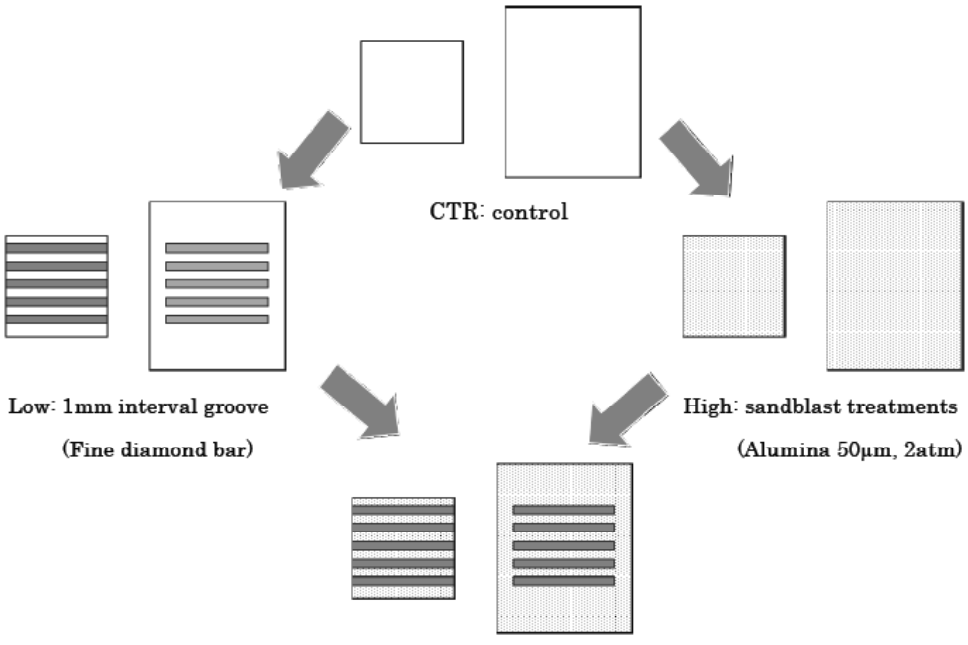

Fig.1 Preparation and procedure of treatments of specimens with surface roughness of the different frequencies (Low, High, Low + High).

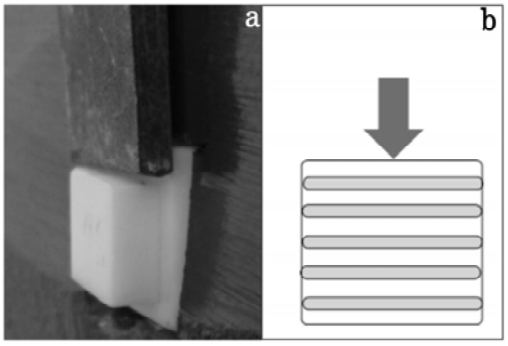

Fig.2 Compression shear bond strength test (a), and the direction of loading on the specimens Low and Low + High (b).

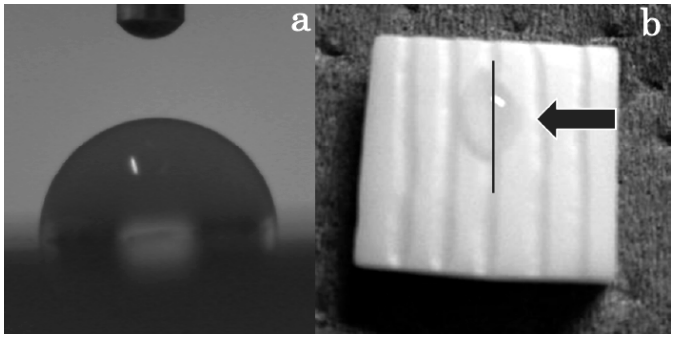

Fig.3 Contact angle measurements (a), and the measurement section for the specimens Low and Low + High (b).

the specimens Low and Low+High, roughness was measured in the vertical direction to the groove (Fig.3b).

4) Fourier analysis: Software of Visual FFT (free soft) and excel (Microsoft, USA) were used for Fourier transform analysis (Fig.6). When $g(x)$ is the original surface roughness profile in real space, the Fourier transform of $g(x)$, the function $G(f)$, is the frequency spectrum, which is the complex variable consisting of a real part (G_r) and imaginary parts (G_i) (eq.1). The power spectrum$|G(f)|$ is used to express the intensity of each frequency peak (eq.2). Function $g(x)$ is the inverse Fourier transform, which is calculated from the real part (G_r) and imaginary parts (G_i) (eq.3). If $G(f)$ is Fourier transformed again (inverse Fourier transform), the original $g(x)$ is obtained. If part of the frequency peaks in $G(f)$, function $H(f)$, is selected, the wave to the selected frequency is reformed in the roughness profile by inverse Fourier transform (eq.4). After the plotting data numbers for measurement length was adapted to the data numbers of 2^n for the Fast Fourier transform analysis, the wavelength was calculated from length and frequency.

5) SEM observation: JSM-6390 (JEOL, Tokyo, Japan) was used for Scanning Electron Microscope (SEM) observation after compression shear bond strength test (Fig.4, 7).

Results

1. Surface roughness

Fig.4 shows the SEM observation of specimen surface. Fig.4a is control, b is sandblast treatments, c is fine diamond bar treatments, and d is fine diamond bar and sandblast treatments. Fig.5 curves of each specimen. Fig.4a is the surface of CTR after sintering with the roughness Ra 0.2 μm as shown in Fig.5a. The scratches formed by mechanical polishing with abrasive paper (#1,500) before sintering can be still observed with a slight contrast. Fig.4b reveals the surface the specimen of High with the high frequency roughness element formed by sandblast treatments with the Ra 0.4 μm (Fig.5b). Fig.4c shows the mechanical striation used to be formed by fine diamond bar inside the groove with the Ra 11 μm in the center to right side (Fig.5c). In Low+High (Fig.4d) with the Ra 13 μm (Fig.5d) the mechanical striation used to be formed by fine diamond bar in the groove

$$G(f) = \int_{-\infty}^{\infty} g(x)\, e^{-2\pi i f x}\, dx = G_r(f) + iG_i(f) \quad (1)$$

$$|G(f)| = \sqrt{G_r(f)^2 + G_i(f)^2} \quad (2)$$

$$g(x) = \int_{-\infty}^{\infty} G(f)\, e^{-2\pi i f x}\, dx = \int_{-\infty}^{\infty} (G_r(f) + iG_i(f))\, e^{-2\pi i f x}\, dx \quad (3)$$

$$h(x) = \int_{-\infty}^{\infty} H(f)\, e^{-2\pi i f x}\, dx = \int_{-\infty}^{\infty} (H_r(f) + iH_i(f))\, e^{-2\pi i f x}\, dx \quad (4)$$

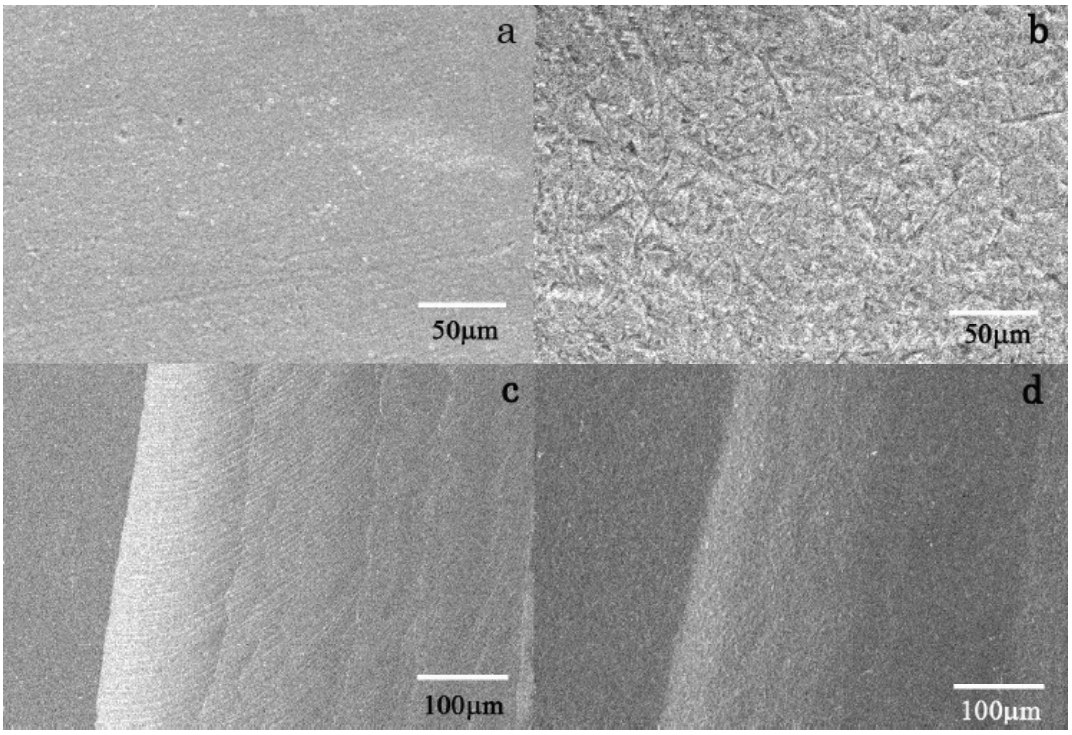

Fig.4 SEM observation of specimen surface a: control, b: sandblast treatments, c: fine diamond bar, d: fine diamond bar and sandblast.

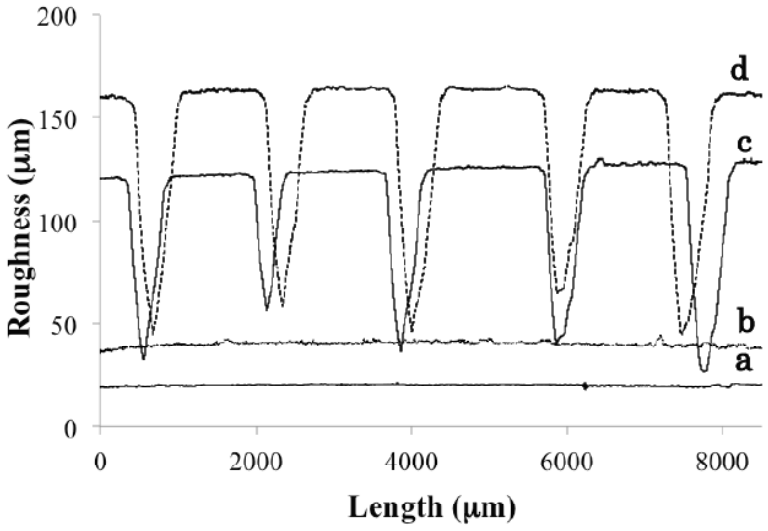

Fig.5 Surface roughness curves of each specimen.
a: CTR (Ra:0.2μm), b: High (0.4μm), c: Low (11μm), d: Low+High (13μm).

before sandblast treatment disappeared and high frequency element by sandblast was observed both on the flat surface and in the groove.

2. Fourier analysis

Fig.6 shows the example of Fourier analysis for the specimen Low+High. Right figures show the real space (surface roughness

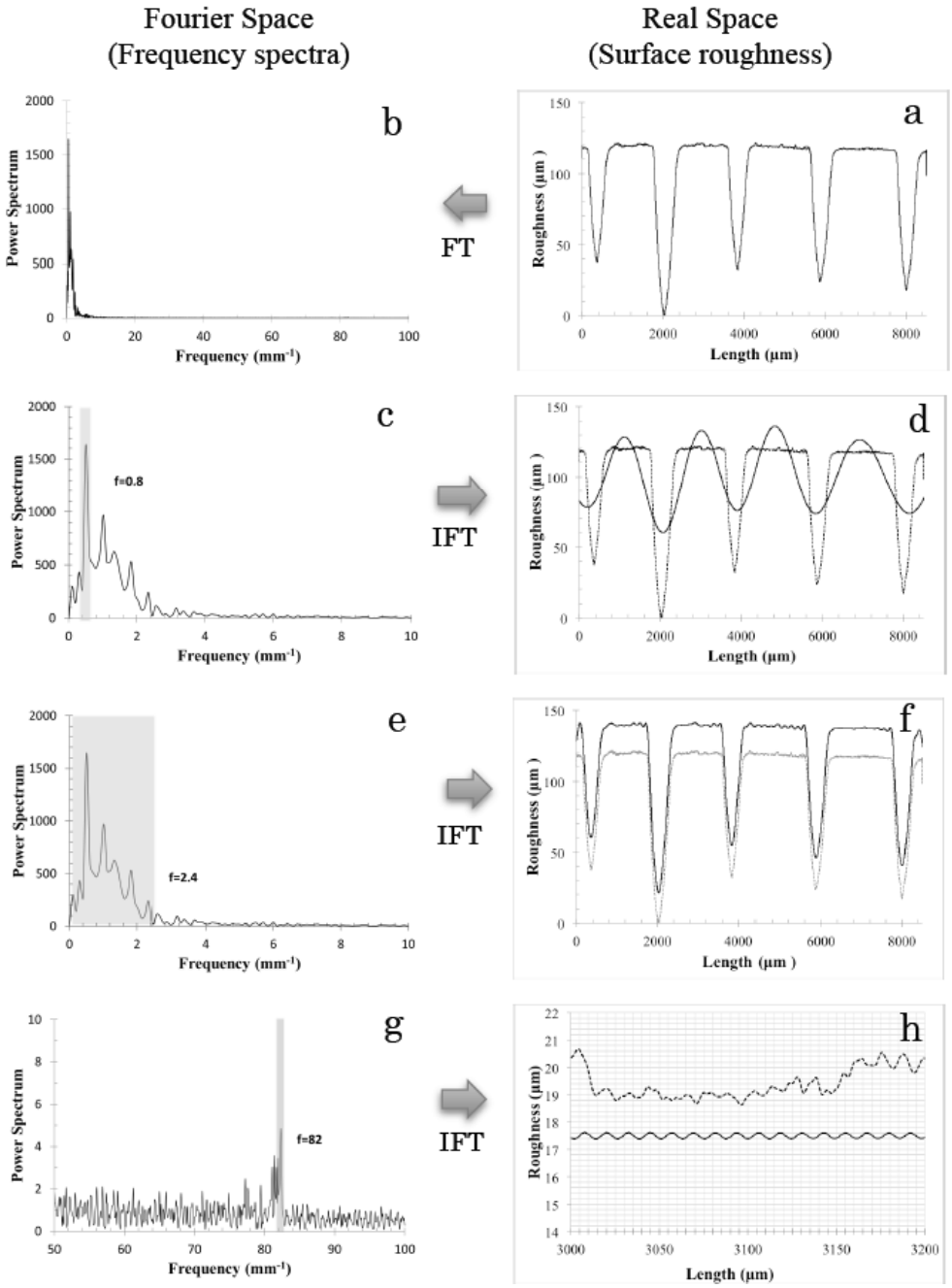

Fig.6 Fourier analysis of the specimen Low+High. Right figures show the real space (surface roughness curves). Left figures show the Fourier space (frequency spectra)

a: Surface roughness profile corresponding to the specimen of Fig.3b and 4b.

b: Frequency spectrum obtained by Fourier transform (FT) of a.

c: Frequency spectrum highlighted with Low-frequency peak at f=0.8mm^{-1}.

d: After inverse Fourier transform (IFT) of the highlighted peak in c. The wavelength (λ=1,600μm) formed from the selected Low-frequency peak is approximately in accordance with the large roughness repetition of original roughness curve (dotted line).

e: Frequency spectrum highlighted with the extended Low-frequency peaks below f=2.4mm^{-1}.

f: After inverse Fourier transform of the highlighted peaks in e. The shape of reformed roughness curve becomes closer to the original curve (dotted line).

g: Frequency spectrum highlighted with High-frequency peak of f=82mm^{-1}.

h: After inverse Fourier transform of the highlighted peak in g. The wavelength (λ=12μm) formed from the selected High-frequency peak in g approximately in accordance with the fine roughness repetition of original curve (dotted line).

curves) and left figures show the Fourier space (frequency spectrum). The roughness curve of Low+High (Fig.6a) could be converted into power spectrum composed of the waves with different frequencies (Fig.6b) by the Fourier transform. The largest peak detected in the low-frequency area was the wave with the frequency 0.8 mm^{-1} (Fig.6 c). After inverse Fourier transform, the curve reformed from the wave of the frequency 0.8 mm^{-1} (bold line) was approximately in accordance with the roughness repetition of original roughness curve (dotted line) (Fig.6 d). After the selection of peaks in the low frequency range was expanded up to the frequency 2.4mm^{-1} (Fig.6e), the roughness curve of inverse Fourier transform becomes much

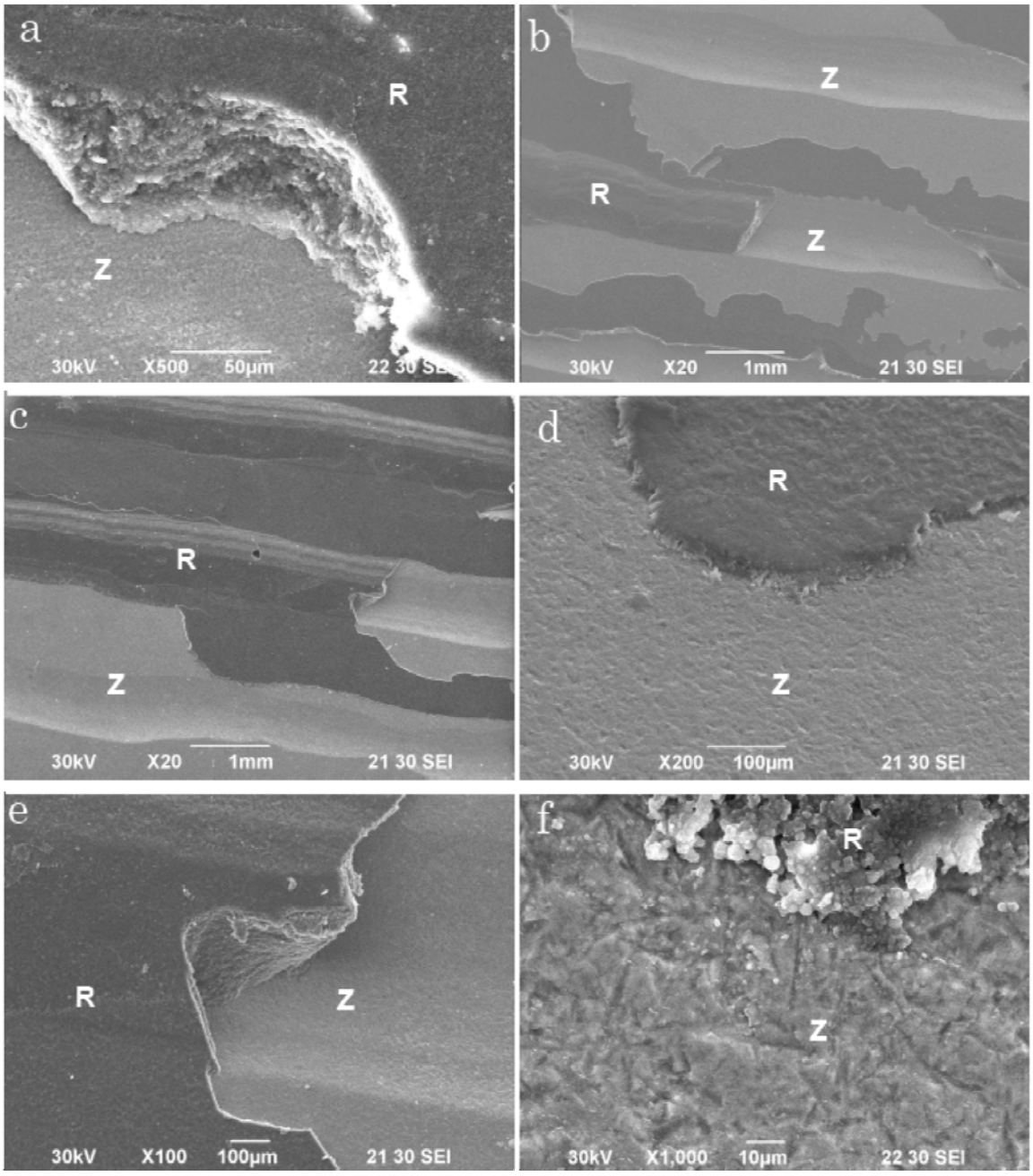

Fig.7 SEM observation of exfoliated surface with resin cement (R) on zirconia (Z) after shear bond strength test. The part with black contrast is the remained resin cement and the bright part is zirconia.
a: CTR, b: Low, c: Low + High, d: High, e: Enlargement of c, f: Enlargement of d.

closer to the original curve (Fig.6f). The largest peak detected in the high-frequency area was the wave of with the frequency 82 mm^{-1} (Fig.6 g). After inverse Fourier transform, the curve re-formed from the wave of the frequency 82mm^{-1} was approximately in accordance with the fine roughness repetition of original roughness curve (Fig.6 h).

Surface characterization formed by each surface treatment was summarized in Table 1 with Ra detected by the surface roughness-measuring instrument and the wavelength λ obtained from Fourier analysis.

Table 1 Summary of surface roughness characterization for each specimen: Average vales of Ra and wavelength.

	Ra (μm)	λ (μm)
CTR	0.2	9800
High	0.4	12
Low	11	1600
Low + High	13	1600+12

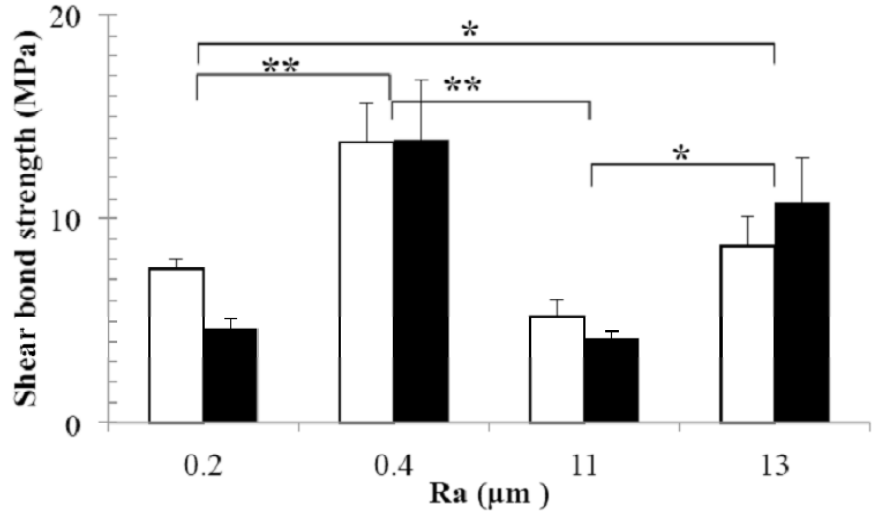

Fig.8 Ra dependence of shear bond strength (White bar: No Primer, Black bar: Primer).

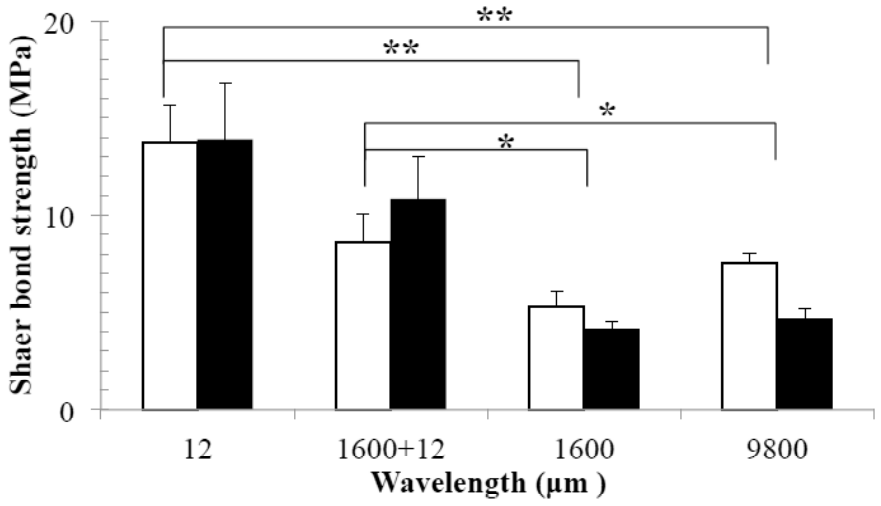

Fig.9 Shear bond strengths in the order of wavelength (White bar: No Primer, Black bar: Primer).

3. SEM observation

Fig.7 shows the SEM observation of exfoliated surface with resin cement on zirconia after shear bond strength test. Fig.7a is CTR, b is Low, c is Low+High, d is High, e is the enlargement of c, and f is the enlargement of d. The part with black contrast was the remained resin cement and the bright part was zirconia. The contrast exhibits the atomic number effect of reflected electrons with the darker contrast for the resin cement composed of light atoms and the brighter contrast for zirconia including the heavy atom Zr. The fracture mode of resin cement was mostly interface fracture. In the fracture surface of resin cement, the filler particles of composite resin structure could be observed (Fig.7a, f). The resin cement remained partially in the trough as low frequency roughness (Fig.7 b, c). In the specimen with a high frequency element, cohesion failure was slightly observed near the boundary line of resin cement and zirconia (Fig, 7f).

4.Compression shear bond strength

Fig.8 shows the Ra dependence of shear bond strength (White bar: No Primer, Black bar: Primer). The result of compression shear bond strength test had the largest for Ra=0.4μm (14MPa), and the smallest for Ra=11μm (4~5MPa). Compression shear bond strength was not in the order of Ra. Shear bond strength was strong in the specimen with a short wavelength (high frequency element), and weak in the specimen with a long wavelength (low frequency element). Shear bond strength was decreasing in the order of wavelength (Fig.9). The mean values of No Primer and Primer were evaluated by Non- repeated Measures ANOVA to compare the difference in Ra (Fig.8) and wavelength (Fig.9) (n=4) (*$p < 0.05$, **$p < 0.001$). The difference of the primer was small.

5.Wettability

Fig.10 shows the contact angle in the order of wavelength. Contact angle with the water for the low frequency roughness element (longer wavelength: λ=1,600μm) has few changes from CTR (80°). Contact angle became smaller (60°) by the high frequency element (shorter wavelength: λ=12μm). All the experimental results were evaluated by Non- repeated Measures ANOVA (n = 10) (**$p < 0.001$).

Discussion

1. Ra and wavelength effect on surface sensitive properties.

Conventionally, as the method to improve adhesive strength, the addition of surface roughness has been done to expect the increase of surface area and interlocking effect. Ra is the most representative value to express surface

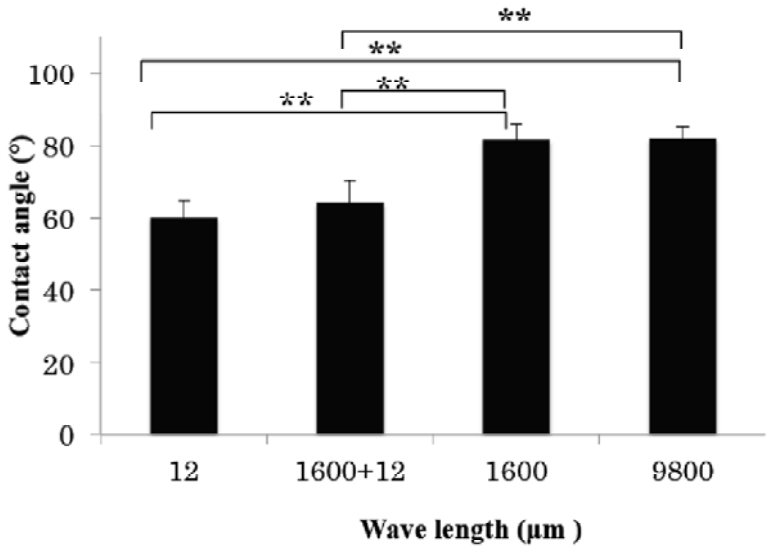

Fig.10 Contact angle in the order of wavelength.

roughness and conventionally Ra dependence for surface sensitive properties such as adhesive strength and contact angle has been widely investigated. In this study Ra increased noticeably by forming the large grooves of low frequency in Low, Low + High, while Ra showed a slight increase by forming the high frequency roughness in High (Fig.5). The shear bond strength of resin cement on zirconia was not well understood by Ra dependence (Fig.8). The periodicity (wavelength) of the roughness in the plane direction looked to have a larger influence, which depends on the surface-sensitive properties. The Fourier transform that can perform frequency analysis was effective to examine the complicated wave pattern and extract the important wave to contribute to the surface sensitive properties, shear bond strength in this case (Fig.6). The shear bond strength showed the tendency to become stronger as the wavelength became shorter (Fig.9). Thus, the evaluation by the wavelength was more appropriate than Ra to interpret the dependence phenomena of compression shear bond strength in the present case.

The effect of primer was not so obvious in this study. This may be due to the wide size of adhesion area, which may easily include the defect and affect the fracture strength, and also the combination of the used resin cement and the primer of the different makers. However there seems more effect in the use of primer for the specimen with the high frequency element.

2.Fracture mode of resin cement on zirconia

SEM observation showed that resin cement partially remained in the groove, which was expected to contribute the large interlocking effect (Fig.7 b, c). Almost all the specimens showed an interface fracture, except that cohesion fracture was slightly observed in part in the specimen with the high frequency roughness (Fig.7 f). These suggest that the adhesive by chemical bond on zirconia is still insufficient and has a room for further improvement. High and Low+High with the high frequency showed the higher bond strength than the roughness of the low frequency (Fig.9).

The surface modulation of the wavelength 12mm obtained by Fourier analysis could be approximately recognized in High on zirconia surface (Fig.7d). Those surface modulations were responsible for the increase of bond strength.

Wettability was improved for high frequency (short wavelength) than low frequency (long wavelength) (Fig.10), which is more appropriate to understand by the wavelength dependence than Ra.

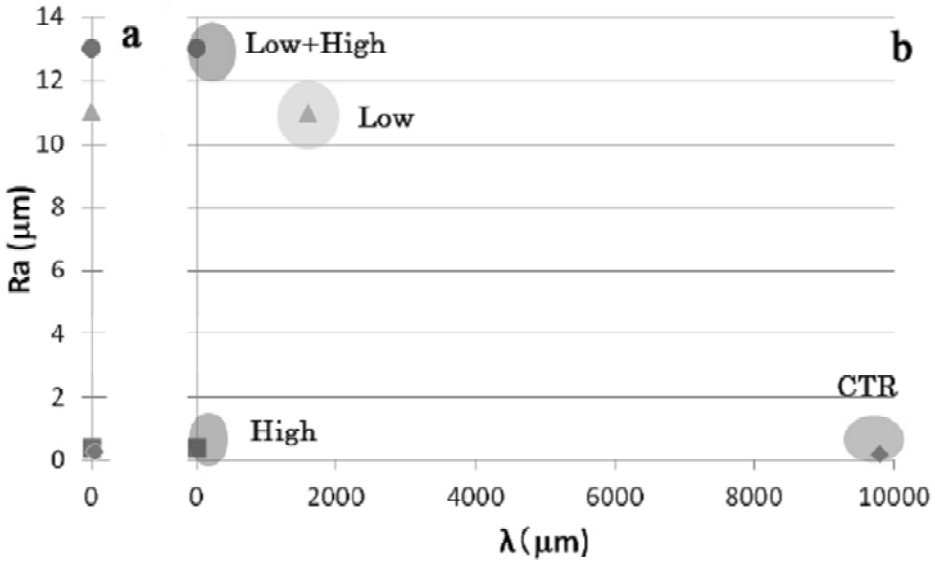

Fig.11 Evaluation conditions of surface roughness properties. a: Ra mono-dependence of surface roughness effect in the conventional researches. b: Ra and wavelength dependence in the present study.

Conclusion

Conventionally, Ra has been mainly used for the evaluation of the surface roughness (Fig.11). In the present study, attention was paid to the dependency not only on Ra but also wavelength. The influence of the wavelength may be more effective than the Ra, depending on the surface sensitive properties. The short wavelength of 10~20 microns contributed more efficiently to the improvement of the bond strength than the big roughness. Analysis using the Fourier transform was effective for various characteristic examinations of the surface-relating properties such as the adhesive strength.

Acknowledgements

We would like to express on sincere thanks to Dr. Norihito Sakaguchi of Faculty of Engineering, Hokkaido University, for the advice on Fourier analysis. We also owe on very important debt to Dr. Seiji Miura of Faculty of Engineering, Hokkaido University, who provided the technical help of shear test. Finally, we would like to thank Mr. Eiji Yamaga of Sapporo Dental Laboratory for his generous grant to complete this study.

References

1) Raigrodski AJ. Contemporary materials and technologies for all-ceramic fixed partial dentures: a review of the literature. J Prosthet Dent 2004; 92:557-562.
2) Watari F, Takashi N, Yokoyama A, Uo M, Akasaka T, Sato Y, Abe S, Totsuka Y, Tohji K. Material nanosizing effect on living organism. J Roy Soc Interface 2009; 6: 371-388.
3) Watari F. Biointeractive and bioreactive nature of nanomaterials, Nano Biomed 2009; 1: 2-8.
4) Kou W, Akasaka T, Watari F, Sjögren G. An in vitro evaluation of the biological effects of carbon nanotube-coated dental zirconia. Hindawi Publishing Corporation 2013:1-6.
5) Furuhashi K, Akasaka T, Kitagawa Y, Watari F. Evaluation of adhesion between material and epithelium using a three-dimensional human epidermal model. Nano Biomed 2012; 4: 76-84.
6) Rosentritt M, Behr M, Bürgers R, Feilzer AJ, Hahnel S. In vitro adherence of oral streptococci to zirconia core and veneering glass-ceramics. J Biomed Mater Res B Appl Biomater 2009;91:257-263.
7) Uo M, Sjögren G, Sundh A, Goto M, Watari F, Bergman M. Effect of surface condition of dental zirconia ceramic (Denzir) on bonding. Dent Mater J 2006;25:626-631.
8) Kawai Y, Uo M, Wang Y, Kono S, Ohnuki S, Watari F. Phase transformation of zirconia ceramics by hydrothermal degradation. Dent Mater J 2011; 30: 286–292.
9) Tarumi N, Uo M, Yamaga E, Watari F. SEM observation and wettability of variously processed and fractured surface of dental zirconia. Appl Surface Sci 2012; 262; 253-257.
10) Konrad-Martin D, Neely ST, Keefe DH, Dorn PA, Gorga MP. Sources of distortion product otoacoustic emissions revealed by suppression experiments and inverse fast Fourier transforms in normal ears. J Acoust Soc Am. 2001 ;109 :2862-2879.
11) Kanamaru T. Introduction to fourier transform: SOFTBANK creative company; 2011.

(Received: November 30, 2013/
Accepted: December 15, 2013)

Corresponding author:
Mr. Naoyoshi Tarumi
2-3-26, Kita24-jonishi, Kita-ku,
Sapporo 001-0024, Japan
Sapporo Dental Laboratory
Tel: +81-11-747-3336
Fax: +81-11-736-3336
E-mail:n_tarumi@sapporo-d.co.jp